



Valproic Acid Induces Autism-Like Synaptic and Behavioral Deficits by Disrupting Histone Acetylation of Prefrontal Cortex ALDH1A1 in Rats

Huan Liu^{1,2}, Mei Tan^{1,2}, Boli Cheng^{1,2}, Si Wang^{1,2}, Lu Xiao^{1,2}, Jiang Zhu^{1,2}, Qionghui Wu^{1,2}, Xi Lai^{1,2}, Qian Zhang^{1,2}, Jie Chen^{1,2*} and Tingyu Li^{1,2*}

¹ Children's Nutrition Research Center, Children's Hospital of Chongqing Medical University, Chongqing, China, ² Chongqing Key Laboratory of Child Nutrition and Health, Ministry of Education Key Laboratory of Child Development and Disorders, National Clinical Research Center for Child Health and Disorder, Chongqing, China

OPEN ACCESS

Edited by:

Li Zhang,

National Institutes of Health (NIH),
United States

Reviewed by:

Vishnu Suppiramaniam,

Auburn University, United States

Hui-Ching Lin,

National Yang-Ming University, Taiwan

*Correspondence:

Jie Chen

jchen010@hospital.cqmu.edu.cn

Tingyu Li

tyli@vip.sina.com

Specialty section:

This article was submitted to

Neuropharmacology,

a section of the journal

Frontiers in Neuroscience

Received: 14 December 2020

Accepted: 06 April 2021

Published: 28 April 2021

Citation:

Liu H, Tan M, Cheng B, Wang S, Xiao L, Zhu J, Wu Q, Lai X, Zhang Q, Chen J and Li T (2021) Valproic Acid Induces Autism-Like Synaptic and Behavioral Deficits by Disrupting Histone Acetylation of Prefrontal Cortex ALDH1A1 in Rats. *Front. Neurosci.* 15:641284. doi: 10.3389/fnins.2021.641284

Objectives: This study aimed to investigate the impact of valproic acid (VPA) on the histone acetylation of acetaldehyde dehydrogenase 1A1 (ALDH1A1) and the mechanism underlying VPA-induced autism-like behavior.

Methods: Female Sprague-Dawley rats were intraperitoneally injected with VPA during gestation to establish an autism model in their offspring. Some offspring prenatally exposed to VPA were randomly treated with MS-275, one histone deacetylase (HDAC) inhibitor, or retinoic acid (RA) after birth. Behavioral tests were conducted on the offspring 6 weeks after birth. Electrophysiological experiments were performed to investigate long-term potentiation (LTP) in the prefrontal cortex (PFC). The expression levels of AMPA receptors (GluA1 and 2), NMDA receptors (GluN1 and 2), synapsin 1 (SYN1), HDAC, acetylated histone 3 (ACh3), RA receptor alpha (RAR α), and ALDH1A1 in the PFC were measured by Western blotting and quantitative polymerase chain reaction. ALDH enzyme activity in PFC tissue was detected using a Micro ALDH Assay Kit. The RA level in the PFC was measured using ultrahigh-performance liquid chromatography/tandem mass spectrometry. A chromatin immunoprecipitation (ChIP) experiment explored the interaction between the ALDH1A1 gene and ACh3.

Results: Offspring prenatally exposed to VPA showed autism-like behavior, upregulated the levels of LTP and GluN2A, GluA1, and SYN1 proteins relevant to synaptic plasticity in the PFC. The expression levels of HDAC3 mRNA and protein were increased. On the other hand, there was a significant reduction in the levels of ACh3, RAR α , RA, ALDH1A1 mRNA and protein, the level of ALDH activity and ACh3 enrichment in the ALDH1A1 promoter region in VPA-induced offspring. Administration of MS-275 in VPA offspring significantly elevated the levels of ACh3, ALDH1A1 mRNA and protein, ALDH activity, RA, the level of RAR α protein and the binding of ACh3 to the ALDH1A1 promoter. In addition, the GluA1 protein level and LTP were reduced, and most behavioral deficits were reversed. After RA supplementation in the VPA-treated offspring, the RA

and RAR α protein levels were significantly upregulated, GluA1 protein and LTP were downregulated, and most autism-like behavioral deficits were effectively reversed.

Conclusion: These findings suggest that VPA impairs histone acetylation of ALDH1A1 and downregulates the RA-RAR α pathway. Such epigenetic modification of ALDH1A1 by VPA leads to autism-like synaptic and behavioral deficits.

Keywords: histone acetylation, ALDH1A1, retinoic acid, RAR α , homeostatic synaptic plasticity, autism spectrum disorder, valproic acid

INTRODUCTION

Autism spectrum disorder (ASD) is a category of neurodevelopmental disorders that are characterized by social and communication impairments and restricted or repetitive behaviors (Sorrell, 2013; Lai et al., 2014). The pathogenesis of ASD is complex, highly heterogeneous, and still unclear (Nicolini and Fahnestock, 2018; Rylaarsdam and Guemez-Gamboa, 2019). Epigenetic abnormalities may be involved in the pathogenesis of multiple ASD subtypes via dysregulation of widespread genes (Ma et al., 2018; Rylaarsdam and Guemez-Gamboa, 2019). Histone deacetylases (HDACs) perform a major epigenetic process by deacetylating histones (Ma et al., 2018) and play pivotal roles in neurodegenerative diseases, including ASD (Guan et al., 2009; Fischer et al., 2010; Gräff et al., 2012; Autism Spectrum Disorders Working Group of The Psychiatric Genomics Consortium, 2017).

Valproic acid (VPA) is a first-line drug for treating refractory epilepsy (Chanda et al., 2019), and it is also a classic HDAC inhibitor (Chanda et al., 2019). Prenatal exposure to VPA increases the risk of cognitive defects and ASD (Rasalam et al., 2005; Koren et al., 2006; Smith and Brown, 2014). The VPA-induced autism animal model may more effectively reflect the heterogeneity of ASD than the autism models caused by single-gene mutations (Nicolini and Fahnestock, 2018). This model has been widely used to explore the neurobiology underlying ASD (Chanda et al., 2019). *In vitro* studies confirmed that VPA causes neurodevelopmental defects primarily via the inhibition of class I HDACs (Chanda et al., 2019). This effect suggests that HDAC activity and the level of histone acetylation may be dysregulated in the VPA-induced autism model. However, the precise mechanism of histone acetylation dysregulation leading to autism-like behaviors is not clear.

Yoshino et al. (2020) reported that the histone acetylation level regulates the expression level of acetaldehyde dehydrogenase 1A1 (ALDH1A1) in the cholangiocarcinoma (Schilderink et al., 2016). ALDH1A1 is a key rate-limiting enzyme that oxidizes retinaldehyde to retinoic acid (RA) (Kumar and Duester, 2011). Studies have shown that RA directly activates the translation of the AMPA receptor subunit GluA1 by binding to extranuclear RA receptors (RAR α) and thus regulates homeostatic synaptic plasticity (HSP) (Maden and Holder, 1991; Clagett-Dame and DeLuca, 2002; Luo et al., 2004; Aoto et al., 2008; Chen and Napoli, 2008; Siegenthaler et al., 2009; Gutierrez-Mazariegos et al., 2011; Chen et al., 2014). HSP dysregulation caused by synaptic structure and function abnormalities is a significant hallmark

of ASD (Bagni and Zukin, 2019). Therefore, we proposed that VPA-induced histone acetylation disorder leads to autism-like synaptic and behavioral deficits via regulation of ALDH1A1-RA-RAR α signaling.

To investigate this hypothesis, we established a VPA-induced autism model in rats. We assessed the changes in HSP, acetylated histone 3 (AcH3) and ALDH1A1-RA-RAR α signaling in the prefrontal cortex (PFC) of VPA-exposed offspring. Then, we used the HDAC inhibitor MS-275 (Simonini et al., 2006) to increase AcH3 levels, induce ALDH1A1-RA-RAR α signaling and rescue autism-like synaptic and behavioral deficits in VPA-exposed offspring. Finally, RA supplementation was used to induce RAR α signaling and improve autism-like synaptic and behavioral deficits in VPA-exposed offspring. The present study first revealed epigenetic modification of ALDH1A1 as a critical mechanism underlying the VPA-induced ASD subtype.

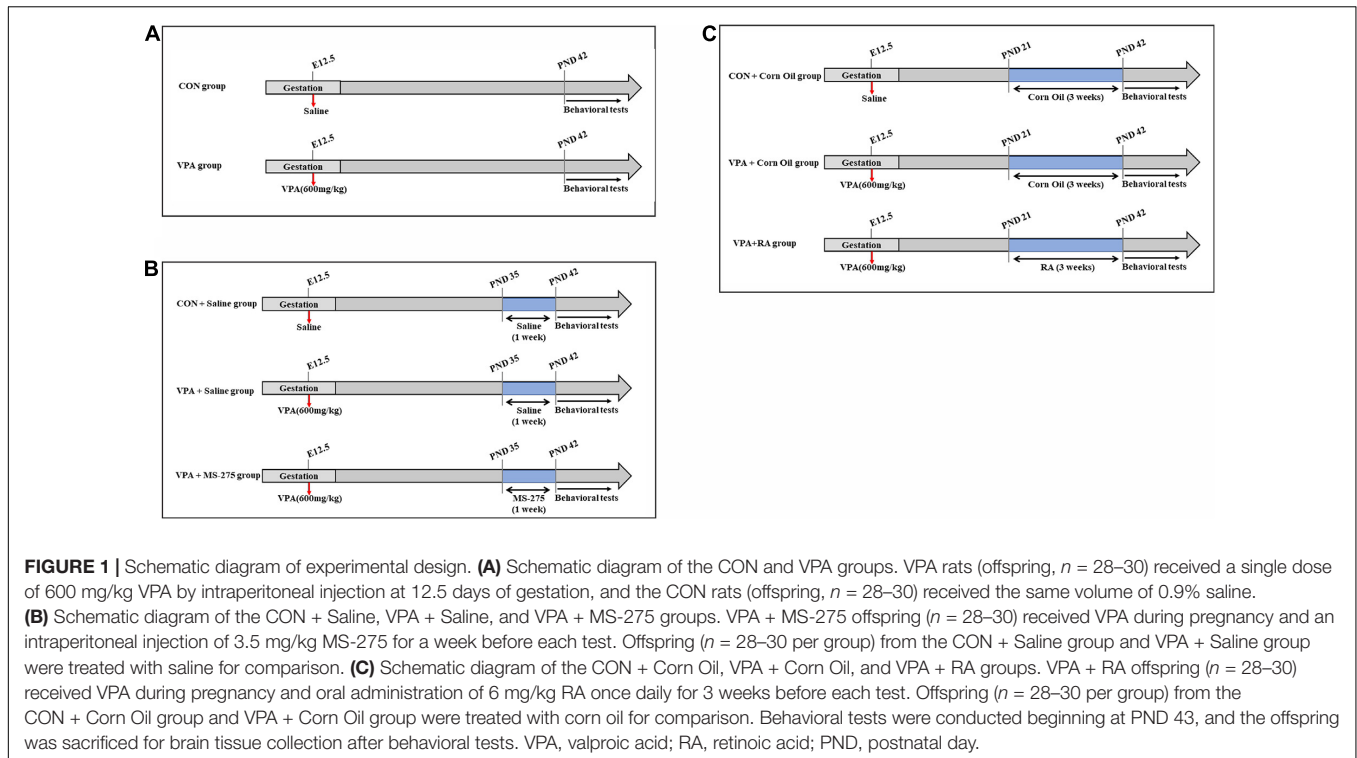
MATERIALS AND METHODS

Animals and Drug Treatment

Sprague-Dawley (SD) rats were obtained from the Animal Care Center of Chongqing Medical University (Chongqing, China) and housed with ad libitum access to food on a 12/12-h light/dark cycle (light: 7 a.m.–7 p.m.; dark: 7 p.m.–7 a.m.). All experiments were approved by the Institutional Animal Care and Use Committee of Chongqing Medical University.

Female adult rats were mated with males. Pregnant rats were randomly assigned to two groups according to random digits: the VPA ($n = 9-10$) group and the control (CON, $n = 9-10$) group (Figure 1A). The pregnant rats in the VPA group were intraperitoneally injected with a single dose of 600 mg/kg VPA (Sigma, diluted to 250 mg/mL with 0.9% saline) at 12.5 days of gestation, and the rats in the CON group were injected with the same volume of 0.9% saline at the same gestational timepoint.

In the MS-275 treatment experiment, female rats were paired with males and randomly assigned to three groups ($n = 9-10$ per group): the CON + Saline group, VPA + Saline group, and VPA + MS-275 group (Figure 1B). The rats in the VPA + Saline group and VPA + MS-275 group were intraperitoneally injected with VPA during pregnancy, and those in the CON + Saline group were injected with saline. Offspring ($n = 28-30$) from the VPA + MS-275 group received an intraperitoneal injection of 3.5 mg/kg MS-275 after birth [AbMole, dissolved in DMSO to make a stock solution (DMSO concentration of the working



solution: < 0.2%) and diluted to 1.5 mg/mL with saline] once daily for 1 week before each test. Offspring ($n = 28-30$ per group) from the CON + Saline group and VPA + Saline group were treated with saline for comparison.

In the RA administration experiment, pregnant female rats were randomly assigned to three groups ($n = 9-10$ per group): the CON + Corn Oil group, VPA + Corn Oil group and VPA + RA group (Figure 1C). The rats in the VPA + Corn Oil and VPA + RA groups were intraperitoneally injected with VPA during pregnancy, and those in the CON + Corn Oil group were treated with saline. Offspring ($n = 28-30$) from the VPA + RA group received an oral administration of 6 mg/kg RA after birth (Sigma, dissolved in corn oil at 2.5 mg/mL) once daily for 3 weeks before each test. Offspring ($n = 28-30$ per group) from the CON + Corn Oil group and VPA + Corn Oil group were treated with corn oil for comparison.

The drug doses and treatment time used were based on previous studies (Ma et al., 2018; Xu et al., 2018; Cheng et al., 2020) and in-house range-finding experiments (see Supplementary Figures 1–5). The offspring used for all experiments in this study were males (Kataoka et al., 2013; Beggiano et al., 2017).

Behavioral Tests

Autism spectrum disorder is characterized by a triad of core defects in social communication, reduced social interactions and stereotyped or repetitive behaviors (Lai et al., 2018; Xu et al., 2018; Cheng et al., 2020). Behavioral tests in animal studies are often needed to assess these autism-like symptoms. The open-field test is used to evaluate repetitive behaviors and the ability

to explore novel environments. The three-chamber social test is used to assess social interaction and social novelty recognition (Deacon, 2006; Xu et al., 2018). Therefore, these two behavioral tests were used in this study, as in most other studies (Lai et al., 2018; Xu et al., 2018; Cheng et al., 2020).

The present study performed behavioral tests with offspring beginning at 6 weeks of age. The open-field test was performed to assess general, exploratory and repetitive behaviors (Deacon, 2006). The total time spent on self-grooming, the time spent in the central zone (the middle square of the 9-square grid), and the total distance traveled during the 5-min test were recorded for each rat. The three-chamber social test was performed to assess social deficits (Deacon, 2006). The apparatus contained three chambers with doorways that allowed access to the side chambers. The test included two phases that lasted 5 min. On the day before the test, the rats were acclimated in the apparatus for 5 min, with an empty cage in each of the two side chambers. The first phase featured an age- and sex-matched stranger rat and an object in the two side chambers, and the second phase contained a stranger rat and a familiar rat in the two side chambers. The time spent in the different chambers was recorded for each test. The apparatus was cleaned after each test. All data were recorded automatically using the ANY-Maze Video Tracking System (Stoelting Co., United States) and analyzed by an experimenter who was blinded to the group assignments.

Animal Tissue Collection

Offspring rats aged approximately 8 weeks were anesthetized and decapitated. PFC tissue was retained. All brain tissues were stored immediately at -80°C .

RNA Extraction and Quantitative Polymerase Chain Reaction (qPCR)

Total RNA was isolated and purified from PFC tissue using an RNA extraction kit (Promega Biotech, China). The Prime Script RT Reagent Kit (Takara, Shiga, Japan) was used to generate cDNA from the tissue mRNA. Real-time qPCR was performed to compare mRNA levels using the SYBR-Green Real-time PCR Kit (Takara) and a CFX96 real-time PCR detection system (Bio-Rad, United States). GAPDH was used as the housekeeping gene to quantitatively analyze the target gene expression, and the mRNA expression level was calculated using the $2^{-\Delta(\Delta CT)}$ method (Ma et al., 2018). Primer sequences for all of the genes profiled in this study were designed using Primer Premier 5 software and are listed below:

GAPDH, sense 5'-CCTGGAGAAACCTGCCAAG-3' and antisense 5'-CACAGGAGACAACCTGGTCC-3'; HDA C1, sense 5'-ATGAAGCCTCACCGA ATCCGAATG-3' and antisense 5'-CTTGGTCATCTCCTCAGCGTTGG-3'; HDAC2, sense 5'-CGAGCATCAGACAAGCGGATAGC-3' and antisense 5'-AGCGACATTCCTACGACCTCCTTC-3'; HDAC3, sense 5'-AACCATGCACCC AGTGTCCA-3' and antisense 5'-TCTCTTCAGCATCGGCCTCG-3'; HD AC8, sense 5'-TGACTGCCAGCCACAGAAGG-3' and antisense 5'-ATGATGCCAC CCTCCAGACCAG-3'; ALD H1A1, sense 5'-ATGTTGACAAAGCTGTGAAGGC-3' and antisense 5'-ACAAGTACGCATTGGCAAAGAC-3'; ALDH1A2, sense 5'-AACTCAGACTTCGGGCTTGAG-3' and antisense 5'-TACTCCCCTAAGCCAA ACTC AC-3'; and ALDH1A3, sense 5'-ATATGTGAGGTGG AAGAAGGCG-3' and antisense 5'-CCATGGTCTCTAG AGTTGCCAG-3'.

Protein Extraction and Western Blotting

Total protein was extracted from PFC tissue using radioimmunoprecipitation assay lysis buffer (KeyGEN, China) containing a 0.1% protease inhibitor cocktail (KeyGEN), and protein concentrations were determined using a BCA protein assay kit (ATGene, China) and a microtiter plate reader (Thermo Fisher Scientific, United States). Nucleoproteins were extracted using the Total Histone Extraction Kit (Epigentek, United States) containing a 0.1% protease inhibitor cocktail, and nucleoprotein concentrations were determined using the Detergent Compatible Bradford Protein Assay Kit (Beyotime, China). Western blotting was performed as previously described (Hou et al., 2015). Briefly, proteins were separated using sodium dodecyl sulfate-polyacrylamide gel electrophoresis (SDS-PAGE) and transferred onto 0.20- μ m polyvinylidene difluoride (PVDF) membranes (Millipore, United States). All membranes were blocked with 5% bovine serum albumin (BSA) (Solarbio, China) in TBST at room temperature for 1 h. The membranes were incubated with primary antibodies at 4°C overnight and secondary antibodies for 1.5 h at room temperature. An enhanced chemiluminescence (ECL) solution (Millipore, United States) was used to detect the immunocomplexes, and the intensity of the bands was analyzed using ImageJ software (National Institutes of Health, Bethesda, Maryland). Primary

antibodies recognizing the following proteins were used for Western blotting (see **Supplementary Table 1**):

GluN1 (1:1000, ab17345, Abcam, RRID: AB_776808), GluN2A (1:1000, 513863, ZENBIO, RRID: AB_2889880), GluN2B (1:1000, ab183942, Abcam, RRID: AB_2889878), GluA1 (1:1000, ab31232, Abcam, RRID: AB_2113447), GluA2 (1:1000, ab133477, Abcam, RRID: AB_2620181), synapsin 1 (SYN1) (1:1000, ab64581, Abcam, RRID: AB_1281135), ACh3 (1:1000, 06599, Sigma, RRID: AB_2115283), Histone 3 (H3) (1:1000, CY6587, Abways, RRID: AB_2889879), RAR α (1:1000, GTX54703, Genetex, RRID: AB_2887874), ALDH1A1 (1:1000, A0157, Abclonal, RRID: AB_2861455), HDAC1 (1:1000, ET1605-35, HuaBio, RRID: AB_2889882), HDAC2 (1:1000, ET1607-78, HuaBio, RRID: AB_2756440), HDAC3 (1:1000, ET1610-5, HuaBio, RRID: AB_2889883), HDAC8 (1:1000, ET1612-90, HuaBio, RRID: AB_2889884), GAPDH (1:5000, HRP60004, Proteintech, RRID: AB_2737588) and PCNA (1:1000, 200947-6B12, ZENBIO, RRID: AB_2722717).

Chromatin Immunoprecipitation (ChIP) and qPCR (ChIP-qPCR)

ChIP was performed using a ChIP kit (Millipore, United States), and PFC tissue samples were prepared as previously described (Hou et al., 2015). Briefly, fresh pretreated PFC tissue was homogenized, and the chromatin was sheared into 200- to 1000-bp fragments by 40 min of medium-power sonication. The chromatin fragments were incubated with 4 μ g of an anti-ACh3 primary antibody (06599, Sigma) or a negative control IgG antibody overnight at 4°C. The specific steps were performed according to the manufacturer's protocols. qPCR was performed using the SYBR-Green Real-time PCR Kit and a CFX96 real-time PCR detection system, as described above. ChIP signals were quantified as fold enrichment using the comparative $\Delta\Delta Ct$ method. A total of seven pairs of primers for sites 0–1000 bp upstream of the rat ALDH1A1 promoter were designed. Only the products amplified with the seventh pair of primers showed significant differences between the CON and VPA groups (data not shown). Therefore, purified DNA was subjected to qPCR with the seventh pair of primers for the ALDH1A1 promoter [sense: 5'-CCCCCTAGCTAAGTCCGA-3', -1035 to -1018 bp relative to the transcription start site (TSS); antisense: 5'-CTGTGTTGATGCTCCTGC-3', -919 to -902 bp relative to the TSS].

Quantitation of RA Using Ultrahigh-Performance Liquid Chromatography/Tandem Mass Spectrometry (UPLC-MS/MS)

As previously reported, all-*trans*-RA levels in the PFC were quantitated using a UPLC-MS/MS method (Xu et al., 2018). Briefly, fresh PFC tissue samples were homogenized with 600 μ l of precooled methanol and 20 μ l of an internal standard (all-*trans*-RA-d6, 100 ng/ml). After centrifugation, the supernatant was transferred to a new centrifuge tube and placed in an

extractor for draining. The sample was redissolved with 50% acetonitrile. The identity of the fraction containing all-*trans*-RA was determined using an Agilent 6470 UPLC-MS/MS system equipped with a unit for atmospheric pressure chemical ionization (APCI) in the positive ion mode. The amounts of all-*trans*-RA in each fraction were quantitated with calibration curves generated from the standard amounts of all-*trans*-RA. All procedures were performed in a dark environment.

ALDH Enzyme Activity Assay

ALDH enzyme activity in PFC tissue was determined using the Micro ALDH Assay Kit (Solarbio, China). After fresh tissue was homogenized, the supernatant was collected for detection of ALDH enzyme activity. One nanomole of NADH produced per minute per milligram of protein was defined as 1 unit of ALDH enzyme activity. The rest of the steps followed the manufacturer's protocols.

Electrophysiology

Eight-week-old rats were anesthetized via intraperitoneal sodium pentobarbital injection (50 mg/kg) and then underwent cardiac perfusion with a 4°C oxygenated cutting solution. After decapitation, brain tissue was removed from the cranial cavity and transferred to the 4°C oxygenated cutting solution. Each liter of cutting solution contained 1.25 mM NaH₂PO₄, 2 mM pyruvate-Na, 26 mM NaHCO₃, 3 mM KCl, 0.4 mM vitamin C, 2 mM lactate-Na, 220 mM sucrose and 10 mM D-glucose. The olfactory bulb and cerebellum were excised, and the remaining brain tissue was glued vertically to a specimen base and fixed in a specimen tank. The PFC was sliced into 400- μ m-thick coronal brain sections using a vibratome. Before recording, the brain sections were incubated in artificial cerebrospinal fluid (ACSF) at 30°C with 95% O₂ and 5% CO₂ for at least 1 h. Each liter of ACSF contained 3 mM KCl, 26 mM NaHCO₃, 2 mM lactate-Na, 124 mM NaCl, 1.25 mM NaH₂PO₄, 0.4 mM vitamin C, 10 mM D-glucose, and 2 mM pyruvate-Na. The stimulation electrode was placed in layer V of the PFC, and the glass recording electrode was placed in layers II-III of the PFC to record the field excitatory postsynaptic potentials (fEPSPs) (Rinaldi et al., 2007; Cui et al., 2011; Xu et al., 2012). The stimulus intensity that elicited 50% of the maximum fEPSP amplitude was used as the test spike intensity, and a recording from a 15-min stable period was used as the baseline. Long-term potentiation (LTP) was induced using high-frequency electrical stimulation (HFS; 100 Hz, 1000 ms) and recorded for 45 min (see **Supplementary Figure 6**; Cui et al., 2011; Hsu et al., 2019). The LTP magnitude was measured as the average potentiation 41–45 min after the onset of HFS induction (Cui et al., 2011; Hsu et al., 2019). Data collection, analyses and processing were performed using pClamp10 software (Molecular Devices).

Statistical Analysis

Data were analyzed using SPSS 20.0 software, and figures were generated using GraphPad Prism 5.0 software. The Shapiro–Wilk test was used to test normality, and Levene's test was used to test the homogeneity of variance. Continuous variables with a normal distribution are presented as the mean \pm SEM.

They were compared using a two-tailed Student's *t*-test (for two-group comparisons) or one-way ANOVA followed by the *post hoc* Bonferroni test (for multiple-group comparisons). Data with a non-normal distribution are shown as the median (P25–P75) in box plots (center line, median; box limits, upper and lower quartiles; whiskers, minimum and maximum values). Non-normal data were analyzed using non-parametric tests (the Mann–Whitney *U* test for two-group comparisons and the Kruskal–Wallis *H* test followed by the *post hoc* Nemenyi test for multiple-group comparisons). To eliminate the influence of sex differences on the results (Kataoka et al., 2013; Beggiato et al., 2017), the offspring used for all experiments in this study were males. Each experiment was repeated at least three times. Statistical significance was set at *P* < 0.05. Based on the study sample size, the effect size and statistical power (1- β err prob) of this study were calculated using *post hoc* analysis with GPower 3.1 software (Ma et al., 2018).

RESULTS

Gestational Exposure to VPA Caused Autism-Like Behavioral Deficits and HSP Dysregulation in the PFC in Offspring

To verify whether prenatal exposure to VPA induces autism-like behaviors, we conducted behavioral tests on offspring, including the open-field and three-chamber social tests (Foley et al., 2012). In the open-field test, there was no noticeable difference in the total distance traveled between the CON and VPA groups, suggesting that VPA exposure does not impair offspring locomotor activity (**Figure 2A**). VPA offspring spent significantly less time in the central zone and more time on self-grooming than CON offspring (**Figures 2B,C**), indicating that VPA exposure increases repetitive behaviors and reduces the ability to explore novel environments. The three-chamber social test using a strange rat and an object as stimuli is called the social interaction test (Deacon, 2006; Xu et al., 2018). The other three-chamber social test using a strange rat and a familiar rat as stimuli is called the social novelty test (Deacon, 2006; Xu et al., 2018). In the social interaction test, CON offspring spent significantly more time in the stranger zone than the object zone, but VPA offspring spent almost equal time between the two zones (**Figure 2D**). In the social novelty test, CON offspring showed more interest in the stranger rat than in the familiar rat, while VPA offspring spent equal time with the two rats (**Figure 2E**). These results indicate that VPA exposure impairs social interaction and social novelty recognition in offspring. These data suggest that prenatal exposure to VPA replicates the core symptoms of autism.

To assess the impact of prenatal exposure to VPA on HSP in offspring, we investigated the expression levels of proteins related to synaptic plasticity, including AMPA receptors (GluA1 and GluA2), NMDA receptors (GluN1, GluN2A and GluN2B) and SYN1, and the level of long-term potentiation (LTP) in the PFC (Zoghbi, 2003; Grant, 2012; Zoghbi and Bear, 2012). Compared to CON offspring, the VPA offspring showed significantly increased GluN2A, GluA1 and SYN1 protein expression levels in the PFC

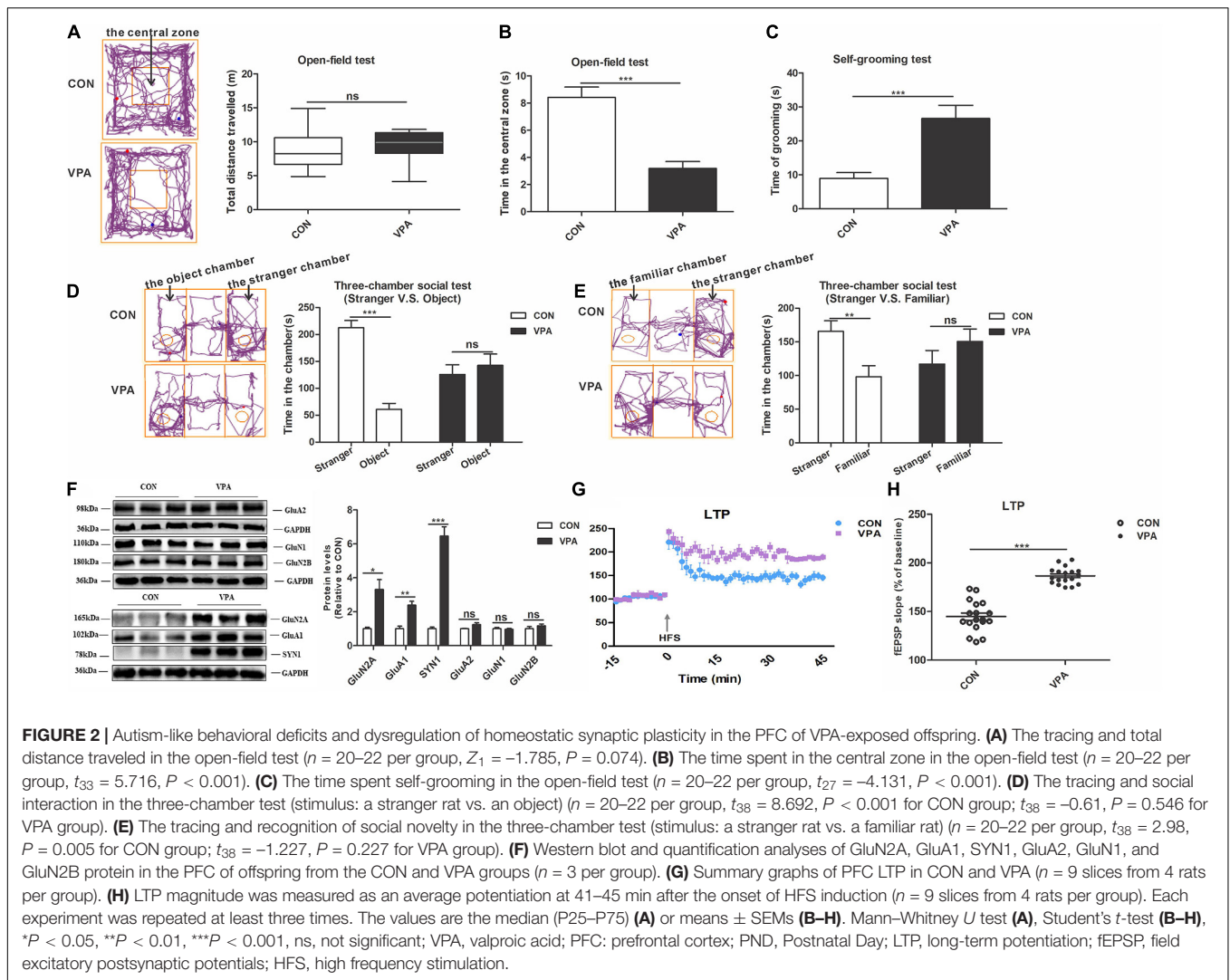


(Figure 2F). However, the levels of GluA2, GluN1, and GluN2B proteins did not change between the VPA and the CON groups (Figure 2F). The electrophysiological experiment performed in the PFC revealed larger LTP in VPA offspring than in CON offspring (Figures 2G,H). These data indicate that VPA exposure may induce HSP dysregulation by regulating the expression of GluA1, GluN2A and SYN1 in offspring.

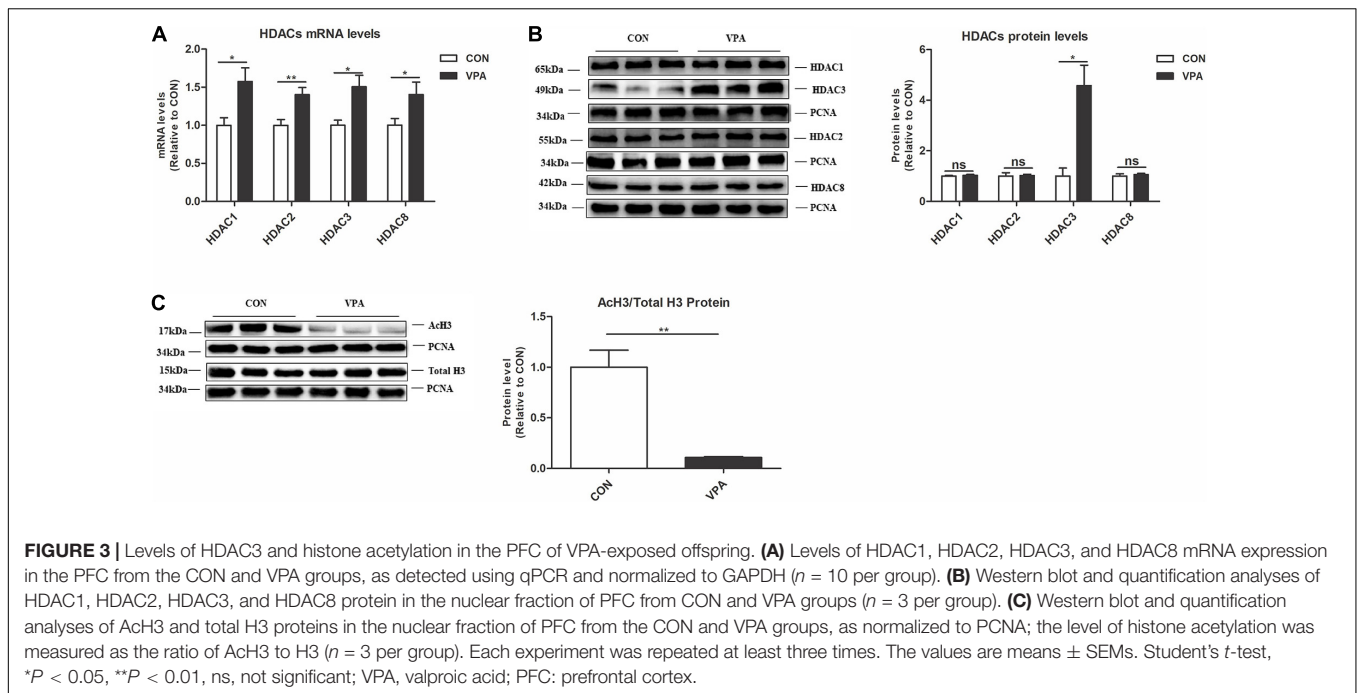
Gestational Exposure to VPA Increased HDAC3 Levels and Downregulated Histone Acetylation Levels in the PFC of Offspring

To identify potential epigenetic aberrations in the VPA-induced autism model, we examined the levels of class I HDACs (HDAC1, HDAC2, HDAC3, and HDAC8) and ACh3 in the PFC nuclear fraction. HDACs are critical enzymes that function in the epigenetic process by deacetylating histones (Ma et al., 2018). The VPA offspring showed significantly higher HDAC1, HDAC2, HDAC3, and HDAC8 mRNA levels and a higher HDAC3 protein

level than the CON offspring (Figures 3A,B). The ratio of ACh3 to H3 in the PFC of offspring was significantly reduced compared to that of CON offspring, indicating the reduction of acetylation level in the VPA offspring (Figure 3C). These data suggest that VPA exposure induces epigenetic abnormalities in histone acetylation in offspring.

Gestational Exposure to VPA Impaired the ALDH1A1-RA-RAR α Pathway in the PFC of Offspring

To investigate the possible molecular mechanisms, we evaluated changes in the ALDH1A1-RA-RAR α pathway in the PFC of VPA-exposed offspring. The RA-RAR α pathway affects HSP and plays a vital role in neurodevelopmental diseases (Aoto et al., 2008; Chen and Napoli, 2008; Zhang et al., 2011; Chen et al., 2014). ALDH1As (ALDH1A1, ALDH1A2, and ALDH1A3) are the key rate-limiting enzymes for RA synthesis (Kumar and Dueter, 2011). Compared to those of CON offspring, the levels of RAR α protein and RA, the levels of ALDH1A1 mRNA and protein, and



the ALDH activity were significantly reduced in the PFC of VPA offspring (Figures 4A–E).

To further investigate the interaction between AcH3 and the ALDH1A1 gene, we conducted a ChIP-qPCR experiment. AcH3 was enriched on the ALDH1A1 gene promoter in the PFC, and this enrichment was significantly decreased in the VPA group compared to the CON group (Figure 4F). These data indicated that the ALDH1A1-RA-RAR α pathway is impaired in the VPA-induced autism model, which might be associated with reduced AcH3.

Treatment With the HDAC Inhibitor MS-275 Rescued the AcH3 Level and the ALDH1A1-RA-RAR α Pathway in the PFC of VPA-Exposed Offspring

To prove that upregulation of the histone acetylation level rescues the impaired ALDH1A1-RA-RAR α pathway, we designed an MS-275 treatment experiment. MS-275 is a brain-region-selective class I HDAC inhibitor that is most potent in the PFC (Ma et al., 2018). Systemic administration of MS-275 significantly restored the level of AcH3 in the PFC of VPA-exposed offspring (Figure 5A). After MS-275 treatment in the VPA offspring, the ALDH1A1 mRNA and protein, ALDH activity, RA, and RAR α protein levels in the PFC were also significantly elevated (Figures 5B–F). These data suggest that MS-275 treatment rescues the AcH3 level and the ALDH1A1-RA-RAR α pathway in the PFC of VPA-exposed offspring.

ChIP-qPCR further showed that MS-275 treatment of VPA-exposed offspring significantly increased the binding of AcH3 to the ALDH1A1 promoter (Figure 5G). This result indicates that AcH3 upregulated the ALDH1A1 expression level via transcription.

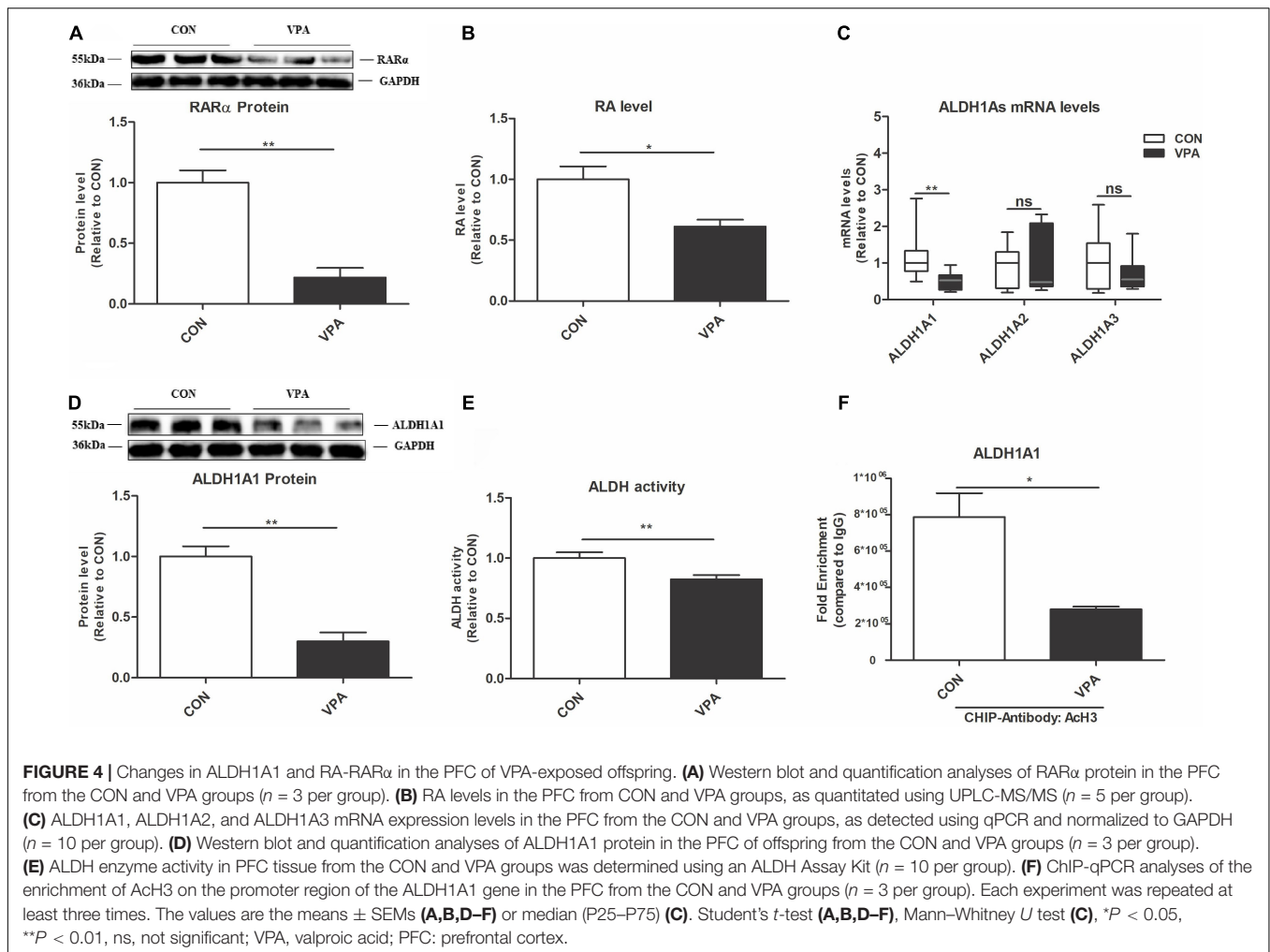
Treatment With the HDAC Inhibitor MS-275 Reversed HSP Deficits and Autism-Like Behavior in VPA-Exposed Offspring

Next, we evaluated the improvement of MS-275 on HSP and autism-like behaviors in VPA offspring. MS-275 administration significantly rescued the abnormal GluA1 level in the PFC of VPA-exposed offspring, and the GluN2A and SYN1 levels did not change (Figure 6A). The electrophysiological experiment showed that MS-275 treatment significantly reduced the abnormally high LTP in VPA-exposed offspring (Figures 6B,C). These data indicate that MS-275 treatment improves the dysregulation of HSP in the PFC of VPA-exposed offspring.

In the open-field test, MS-275 treatment of VPA offspring significantly increased the central zone's time and did not affect the total distance traveled and self-grooming time (Figures 6D–F). In the social interaction test, VPA-exposed offspring treated with MS-275 exhibited a significantly stronger preference for the stranger rat over the object (Figure 6G). In the social novelty test, VPA offspring treated with MS-275 spent equal time with the stranger and familiar rats (Figure 6H). These results suggest that MS-275 partially rescues autism-like behavioral deficits of VPA offspring, such as the abilities to explore novel objects and participate in social interactions.

Upregulation of RA-RAR α Pathway Restored HSP Dysregulation and Autism-Like Behavioral Deficits in VPA-Exposed Offspring

To further study the causative role of the RA-RAR α pathway in the VPA-induced autism model, we designed an RA treatment



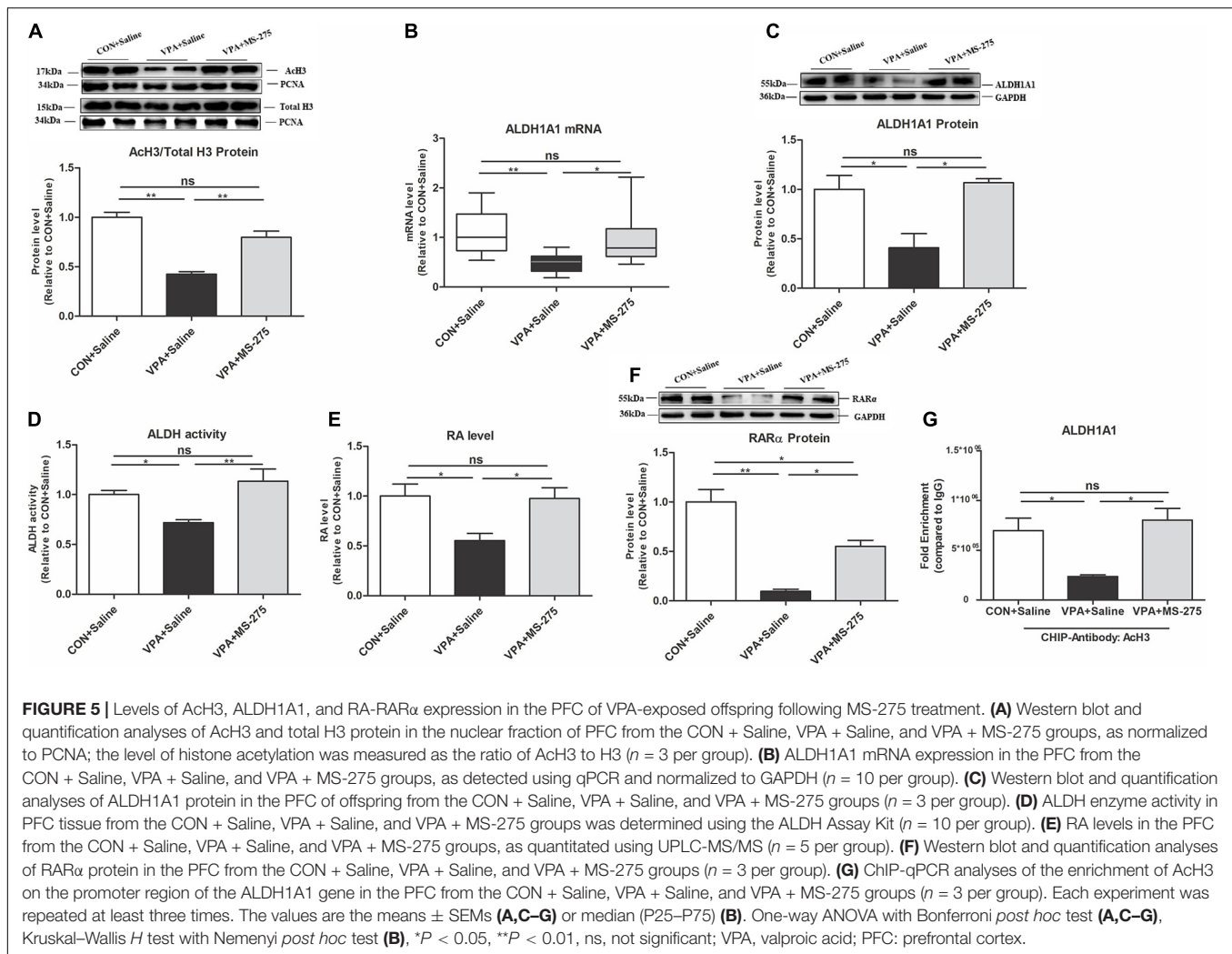
experiment. Administration of RA significantly enhanced RA and RAR α levels in the PFC of VPA offspring (**Figures 7A,B**). The ALDH1A1, Ach3, and HDAC3 levels were not significantly changed after RA treatment (data not shown).

We then explored the effect of RA treatment on the HSP and autism-like behavior in VPA-exposed offspring. The level of GluA1 was significantly reduced in VPA offspring treated with RA (**Figure 7C**). The Electrophysiological experiment in the PFC showed that RA treatment reduced the LTP level in VPA-exposed offspring (**Figures 7D,E**). These data indicate that the recovery of RA-RAR α pathway rescues impaired HSP in the PFC of VPA-exposed offspring. In the open-field test, RA treatment of VPA offspring significantly increased the central zone's time and did not change the total distance traveled and self-grooming time (**Figures 7F–H**). In the three-chamber social test, VPA offspring treated with RA spent more time with the stranger rat over the object and showed a stronger preference for the stranger rat over the familiar rat (**Figures 7I,J**). These results suggest that RA partially restores autism-like behavioral deficits in VPA offspring, such as the abilities to explore novel things, participate in social interaction and recognize social novelty.

DISCUSSION

Prenatal VPA exposure is an apparent risk factor for ASD, and the VPA-induced autism model is a classic model for studying the neurobiology underlying ASD (Mabunga et al., 2015). Our study showed that prenatal exposure to VPA replicates the core symptoms of autism, suggesting that the VPA-induced autism model was successfully constructed. Recent studies have validated HSP dysregulation as a major hallmark of ASD (Bagni and Zukin, 2019). AMPA receptors (GluA1 and GluA2), NMDA receptors (GluN1 and GluN2) and SYN1 are critical molecular markers of synaptic plasticity, and LTP is an essential form of synaptic plasticity (Bagni and Zukin, 2019). Our study found the widely upregulated protein levels (GluN2A, GluA1, and SYN1) and enhanced LTP in the PFC of VPA-exposed offspring, consistent with previous reports (Rinaldi et al., 2007; Markram et al., 2008). These results indicate that HSP dysregulation caused by GluN2A, GluA1, and SYN1 aberrants is a vital pathological feature of the VPA-induced autism model.

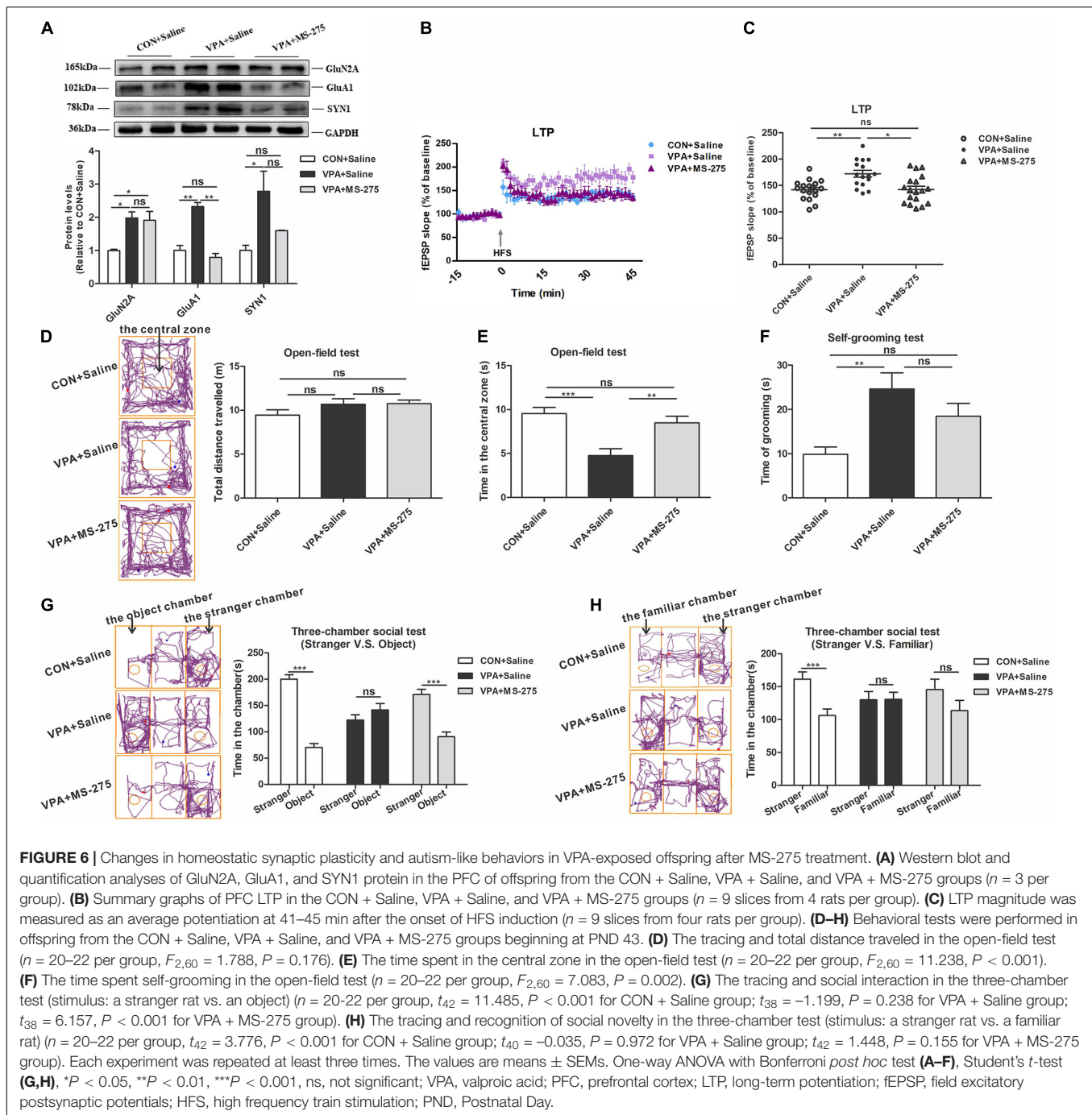
Epigenetic modification is important in the heterogeneous pathogenesis of ASD (Ma et al., 2018; Rylaarsdam and Guemez-Gamboa, 2019). HDACs perform a major epigenetic process by



deacetylating histones (Ma et al., 2018) and play pivotal roles in neurodegenerative diseases, including ASD (Guan et al., 2009; Fischer et al., 2010; Gräff et al., 2012; Autism Spectrum Disorders Working Group of The Psychiatric Genomics Consortium, 2017). VPA inhibits HDAC activity and impairs histone acetylation (Phiel et al., 2001; Kazantsev and Thompson, 2008), which may be responsible for VPA-induced teratogenesis (Phiel et al., 2001), birth defects (Phiel et al., 2001) and even autism-like behaviors. One previous study found that prenatal VPA exposure caused a transient increase in acetylated histone levels in the embryonic brain, which may be due to the direct inhibitory effect of VPA on HDAC activity (Kataoka et al., 2013). However, our study observed that VPA exposure reduced the ACh3 level in the postnatal brain in offspring, consistent with the report by Kazlauskas et al. (2016). It is speculated that prenatal VPA exposure indirectly induces the overexpression of HDACs via negative feedback, leading to an imbalance in epigenetic regulation. The increased HDAC expression in VPA offspring in our study also confirmed this speculation. The reasons for the upregulation of HDAC levels must be further studied. All

these findings suggest that dysfunction in acetylation epigenetics may be closely involved in the pathogenesis of VPA-induced autism-like behaviors.

To identify the precise mechanisms of epigenetic modification, we also examined the change in the ALDH1A1-RA-RAR α pathway in the PFC of the VPA-induced autism model. The RA-RAR α pathway regulates the expression of proteins associated with synaptic plasticity, such as GluA1, and plays a critical causative role in neurological diseases (Aoto et al., 2008; Chen and Napoli, 2008; Chen et al., 2014). ALDH1A family proteins are key rate-limiting enzymes in RA synthesis (Kumar and Duester, 2011; Zhang et al., 2017). Some studies have found that variants in the ALDH1A family genes are clinically related to ASD (Galter et al., 2003; Wan et al., 2009; Fares-Taie et al., 2013). Another report confirmed that administration of an ALDH1A antagonist induced autism-like symptoms in mice (Xu et al., 2018). Our study showed a reduction of ALDH1A1 level and ALDH activity in VPA-exposed offspring, consistent with the decreased RA and RAR α protein levels. These results indicate that decreased



ALDH1A1-RA-RAR α pathway might play a key role in the VPA-induced autism model. Previous studies have reported that histone acetylation levels regulate ALDH1A1 expression levels via transcription in cholangiocarcinoma (Schilderink et al., 2016; Yoshino et al., 2020). Our ChIP-qPCR experiment showed that AcH3 enrichment on the ALDH1A1 gene promoter was decreased in the PFC of VPA offspring. Considering the parallel downregulation of AcH3, AcH3 enrichment and ALDH1A1 levels, we hypothesized that the decreased ALDH1A1 levels may be associated with reduced AcH3.

The causal regulatory relationship between AcH3 and ALDH1A1 was studied. We observed that HDAC inhibitor MS-275 treatment of VPA offspring increased acetylation levels, followed by the upregulation of ALDH1A1 level. The impaired RA-RAR α pathway and most autism-like synaptic and behavioral deficits were also significantly rescued. ChIP-qPCR further showed that AcH3 enrichment on the ALDH1A1 gene promoter after MS-275 treatment was elevated, consistent with the upregulation of the ALDH1A1 level. Together, these results clarify that the decreased histone acetylation downregulates

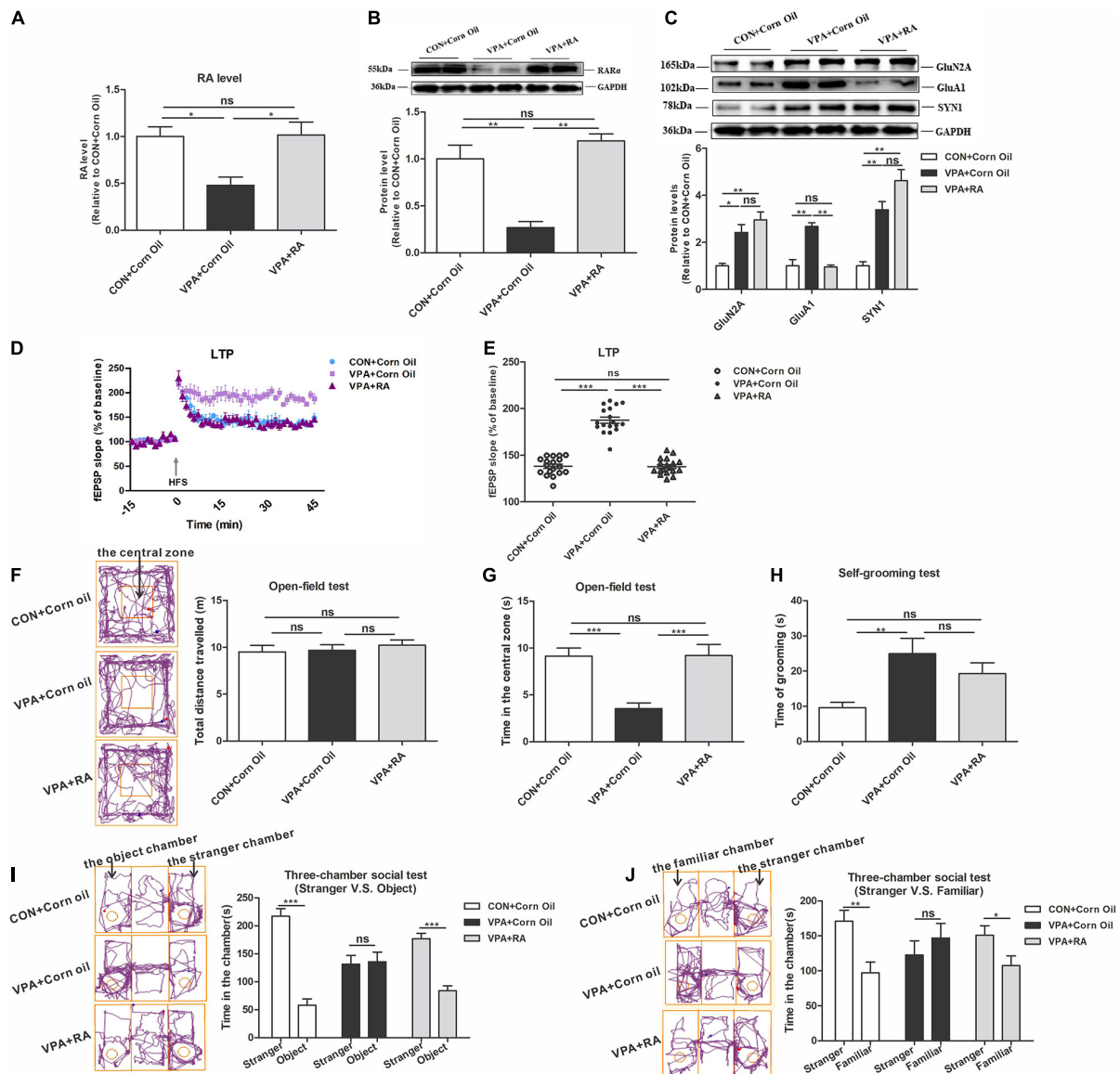


FIGURE 7 | Changes in RAR α expression levels, homeostatic synaptic plasticity and autism-like behaviors in VPA-exposed offspring following RA intervention. **(A)** RA levels in the PFC from the CON + Corn Oil, VPA + Corn Oil, and VPA + RA groups, as quantitated using UPLC-MS/MS ($n = 5$ per group). **(B)** Western blot and quantification analyses of RAR α protein in the PFC from the CON + Corn Oil, VPA + Corn Oil, and VPA + RA groups ($n = 3$ per group). **(C)** Western blot and quantification analyses of GluN2A, GluA1, and SYN1 protein in the PFC of offspring from the CON + Corn Oil, VPA + Corn Oil, and VPA + RA groups ($n = 3$ per group). **(D)** Summary graphs of PFC LTP in the CON + Corn Oil, VPA + Corn Oil, and VPA + RA groups ($n = 9$ slices from four rats per group). **(E)** LTP magnitude was measured as an average potentiation at 41–45 min after the onset of HFS induction ($n = 9$ slices from four rats per group). **(F–J)** Behavioral tests were performed in offspring from the CON + Corn Oil, VPA + Corn Oil, and VPA + RA groups beginning at PND 43. **(F)** The tracing and total distance traveled in the open-field test ($n = 20–22$ per group, $F_{2,57} = 0.356$, $P = 0.702$). **(G)** The time spent in the central zone in the open-field test ($n = 20–22$ per group, $F_{2,57} = 12.511$, $P < 0.001$). **(H)** The time spent self-grooming in the open-field test ($n = 20–22$ per group, $F_{2,58} = 5.709$, $P = 0.005$). **(I)** The tracing and social interaction in the three-chamber test (stimulus: a stranger rat vs. an object) ($n = 20–22$ per group, $t_{38} = 9.079$, $P < 0.001$ for CON + Corn Oil group; $t_{38} = -0.191$, $P = 0.85$ for VPA + Corn Oil group; $t_{42} = 7.214$, $P < 0.001$ for VPA + RA group). **(J)** The tracing and recognition of social novelty in the three-chamber test (stimulus: a stranger rat vs. a familiar rat) ($n = 20–22$ per group, $t_{38} = 3.366$, $P = 0.002$ for CON + Corn Oil group; $t_{38} = -0.836$, $P = 0.408$ for VPA + Corn Oil group; $t_{40} = 2.243$, $P = 0.031$ for VPA + RA group). Each experiment was repeated at least three times. The values are means \pm SEMs. One-way ANOVA with Bonferroni *post hoc* test **(A–H)**, Student's *t*-test **(I, J)**, * $P < 0.05$, ** $P < 0.01$, *** $P < 0.001$, ns = not significant; VPA, valproic acid; PFC, prefrontal cortex; RA, retinoic acid; LTP, long-term potentiation; fEPSP, field excitatory postsynaptic potentials; HFS, high frequency train stimulation; PND, postnatal day.

ALDH1A1 expression via transcription and impairs the RA-RAR α pathway, thereby leading to autism-like synaptic and behavioral deficits in VPA-exposed offspring.

Subsequently, in the RA treatment experiment, we demonstrated that the RA-RAR α pathway upregulation reduced GluA1 level and HSP, thereby partially rescuing most autism-like

behaviors in VPA-exposed offspring. The ALDH1A1 and AcH3 levels were not changed after RA treatment (data not shown). These results fully prove that the RA-RAR α pathway plays a critical causative role downstream of ALDH1A1 in the VPA-induced autism model. Xu et al. (2018) also identified impaired RA homeostasis as a key mechanism underlying the UBE3A hyperactivity-induced autism model. In their autism model, RA reduction decreased the binding to RAR α and elevated the binding of RAR α to GluA1 mRNA without impairing the RAR α level, which reduced GluA1 translation and HSP (Poon and Chen, 2008; Xu et al., 2018). In our study, the increase in HSP might be due to the downregulation of RAR α , which reduced the binding of RAR α to GluA1 mRNA and thus increased GluA1 translation (Poon and Chen, 2008; Hsu et al., 2019).

Notably, Foley et al. (2012) and our studies both found that HDAC inhibitors improved VPA-induced autism-like behavioral deficits via HSP restoration. HDAC inhibitors also showed significant therapeutic effects on behavioral deficits in the Shank3-deficient autism model via HSP regulation (Ma et al., 2018). These results suggest that HDAC-targeting agents have great potential for the treatment heterogeneous autism due to their extensive regulatory effects on HSP (Ma et al., 2018). This provides new ideas for the treatment of ASD and is worthy of in-depth study.

One limitation of our study was that autism-like synaptic and behavioral deficits were not wholly remedied by MS-275 treatment, suggesting that there may be other pathogenic mechanisms in the VPA-induced autism model.

CONCLUSION

Our study first found that VPA caused autism-like synaptic and behavioral deficits by impairing the histone acetylation of ALDH1A1 and thus downregulating the RA-RAR α pathway, suggesting a precise epigenetic mechanism underlying the VPA-induced autism model. Synaptic and behavioral deficits were significantly rescued by regulating the histone acetylation of ALDH1A.

DATA AVAILABILITY STATEMENT

The raw data supporting the conclusions of this article will be made available by the authors, without undue reservation.

REFERENCES

- Aoto, J., Nam, C. I., Poon, M. M., Ting, P., and Chen, L. (2008). Synaptic signaling by all-trans retinoic acid in homeostatic synaptic plasticity. *Neuron* 60, 308–320. doi: 10.1016/j.neuron.2008.08.012
- Autism Spectrum Disorders Working Group of The Psychiatric Genomics Consortium (2017). Meta-analysis of GWAS of over 16,000 individuals with autism spectrum disorder highlights a novel locus at 10q24.32 and a significant overlap with schizophrenia. *Mol. Autism* 8:21. doi: 10.1186/s13229-017-0137-9

ETHICS STATEMENT

The animal study was reviewed and approved by the Animal Experimentation Ethics Committee of Chongqing Medical University (Chongqing, China) and conducted in accordance with the guidelines of the Institutional Animal Care and Use Committee of Chongqing Medical University.

AUTHOR CONTRIBUTIONS

HL: methodology, investigation, formal analysis, and writing an original draft. MT: investigation, software, and formal analysis. BC: investigation and software. SW, LX, JZ, QW, XL, and QZ: investigation. JC: conceptualization, methodology, supervision, validation, writing – review and editing. TL: conceptualization, funding acquisition, supervision, validation, writing – review and editing. All authors contributed to the article and approved the submitted version.

FUNDING

This work was supported by the National Natural Science Foundation of China (81770526, 31971089) from JC, and the National Natural Science Foundation of China (81771223), the Key Scientific and Technological Projects of Guangdong Province (2018B030335001) and Guangzhou City (202007030002) from TL.

ACKNOWLEDGMENTS

We would like to thank Professor Chen Hengsheng from the pediatrics Research Institute of Children's Hospital, affiliated with Chongqing Medical University, for his guidance and assistance in electrophysiological technology.

SUPPLEMENTARY MATERIAL

The Supplementary Material for this article can be found online at: <https://www.frontiersin.org/articles/10.3389/fnins.2021.641284/full#supplementary-material>

- Bagni, C., and Zukin, R. S. (2019). A Synaptic perspective of fragile x syndrome and autism spectrum disorders. *Neuron* 101, 1070–1088. doi: 10.1016/j.neuron.2019.02.041
- Beggiato, A., Peyre, H., Maruani, A., Scheid, I., Rastam, M., Amsellem, F., et al. (2017). Gender differences in autism spectrum disorders: Divergence among specific core symptoms. *Autism Res.* 10, 680–689. doi: 10.1002/aur.1715
- Chanda, S., Ang, C. E., Lee, Q. Y., Ghebrial, M., Haag, D., Shibuya, Y., et al. (2019). Direct reprogramming of human neurons identifies MARCKSL1 as a pathogenic mediator of valproic acid-induced teratogenicity. *Cell Stem Cell* 25, 103–119.e106. doi: 10.1016/j.stem.2019.04.021

- Chen, L., Lau, A. G., and Sarti, F. (2014). Synaptic retinoic acid signaling and homeostatic synaptic plasticity. *Neuropharmacology* 78, 3–12. doi: 10.1016/j.neuropharm.2012.12.004
- Chen, N., and Napoli, J. L. (2008). All-trans-retinoic acid stimulates translation and induces spine formation in hippocampal neurons through a membrane-associated RARalpha. *FASEB J.* 22, 236–245. doi: 10.1096/fj.07-8739com
- Cheng, B., Zhu, J., Yang, T., Wang, S., Liu, H., Wu, Q., et al. (2020). Vitamin A deficiency exacerbates autism-like behaviors and abnormalities of the enteric nervous system in a valproic acid-induced rat model of autism. *Neurotoxicology* 79, 184–190. doi: 10.1016/j.neuro.2020.06.004
- Clagett-Dame, M., and DeLuca, H. F. (2002). The role of vitamin A in mammalian reproduction and embryonic development. *Annu. Rev. Nutr.* 22, 347–381. doi: 10.1146/annurev.nutr.22.010402.102745E
- Cui, Y., Jin, J., Zhang, X., Xu, H., Yang, L., Du, D., et al. (2011). Forebrain NR2B overexpression facilitating the prefrontal cortex long-term potentiation and enhancing working memory function in mice. *PLoS One* 6:e20312. doi: 10.1371/journal.pone.0020312
- Deacon, R. M. (2006). Housing, husbandry and handling of rodents for behavioral experiments. *Nat. Protoc.* 1, 936–946. doi: 10.1038/nprot.2006.120
- Fares-Taie, L., Gerber, S., Chassaing, N., Clayton-Smith, J., Hanein, S., Silva, E., et al. (2013). ALDH1A3 mutations cause recessive anophthalmia and microphthalmia. *Am. J. Hum. Genet.* 92, 265–270. doi: 10.1016/j.ajhg.2012.12.003
- Fischer, A., Sananbenesi, F., Mungenast, A., and Tsai, L. H. (2010). Targeting the correct HDAC(s) to treat cognitive disorders. *Trends Pharmacol. Sci.* 31, 605–617. doi: 10.1016/j.tips.2010.09.003
- Foley, A. G., Gannon, S., Rombach-Mullan, N., Prendergast, A., Barry, C., Cassidy, A. W., et al. (2012). Class I histone deacetylase inhibition ameliorates social cognition and cell adhesion molecule plasticity deficits in a rodent model of autism spectrum disorder. *Neuropharmacology* 63, 750–760. doi: 10.1016/j.neuropharm.2012.05.042
- Galter, D., Buervenich, S., Carmine, A., Anvret, M., and Olson, L. (2003). ALDH1 mRNA: presence in human dopamine neurons and decreases in substantia nigra in Parkinson's disease and in the ventral tegmental area in schizophrenia. *Neurobiol. Dis.* 14, 637–647. doi: 10.1016/j.nbd.2003.09.001
- Gräff, J., Rei, D., Guan, J. S., Wang, W. Y., Seo, J., Hennig, K. M., et al. (2012). An epigenetic blockade of cognitive functions in the neurodegenerating brain. *Nature* 483, 222–226. doi: 10.1038/nature10849
- Grant, S. G. (2012). Synaptopathies: diseases of the synaptome. *Curr. Opin. Neurobiol.* 22, 522–529. doi: 10.1016/j.conb.2012.02.002
- Guan, J. S., Haggarty, S. J., Giacometti, E., Dannenberg, J. H., Joseph, N., Gao, J., et al. (2009). HDAC2 negatively regulates memory formation and synaptic plasticity. *Nature* 459, 55–60. doi: 10.1038/nature07925
- Gutierrez-Mazariegos, J., Theodosiou, M., Campo-Paysaa, F., and Schubert, M. (2011). Vitamin A: a multifunctional tool for development. *Semin. Cell Dev. Biol.* 22, 603–610. doi: 10.1016/j.semcdb.2011.06.001
- Hou, N., Ren, L., Gong, M., Bi, Y., Gu, Y., Dong, Z., et al. (2015). Vitamin A deficiency impairs spatial learning and memory: the mechanism of abnormal CBP-dependent histone acetylation regulated by retinoic acid receptor alpha. *Mol. Neurobiol.* 51, 633–647. doi: 10.1007/s12035-014-8741-6
- Hsu, Y. T., Li, J., Wu, D., Südhof, T. C., and Chen, L. (2019). Synaptic retinoic acid receptor signaling mediates mTOR-dependent metaplasticity that controls hippocampal learning. *Proc. Natl. Acad. Sci. U.S.A.* 116, 7113–7122. doi: 10.1073/pnas.1820690116
- Kataoka, S., Takuma, K., Hara, Y., Maeda, Y., Ago, Y., and Matsuda, T. (2013). Autism-like behaviours with transient histone hyperacetylation in mice treated prenatally with valproic acid. *Int. J. Neuropsychopharmacol.* 16, 91–103. doi: 10.1017/s1461145711001714
- Kazantsev, A. G., and Thompson, L. M. (2008). Therapeutic application of histone deacetylase inhibitors for central nervous system disorders. *Nat. Rev. Drug Discov.* 7, 854–868. doi: 10.1038/nrd2681
- Kazlauskas, N., Campolongo, M., Lucchina, L., Zappala, C., and Depino, A. M. (2016). Postnatal behavioral and inflammatory alterations in female pups prenatally exposed to valproic acid. *Psychoneuroendocrinology* 72, 11–21. doi: 10.1016/j.psyneuen.2016.06.001
- Koren, G., Nava-Ocampo, A. A., Moretti, M. E., Sussman, R., and Nulman, I. (2006). Major malformations with valproic acid. *Can. Fam. Physician* 52, 441–447.
- Kumar, S., and Duester, G. (2011). SnapShot: retinoic acid signaling. *Cell* 147, 1422–1422.e1421. doi: 10.1016/j.cell.2011.11.034
- Lai, M. C., Lombardo, M. V., and Baron-Cohen, S. (2014). Autism. *Lancet* 383, 896–910. doi: 10.1016/s0140-6736(13)61539-1
- Lai, X., Wu, X., Hou, N., Liu, S., Li, Q., Yang, T., et al. (2018). Vitamin A deficiency induces autistic-like behaviors in rats by regulating the RARβ-CD38-oxytocin axis in the hypothalamus. *Mol. Nutr. Food Res.* 62:1700754. doi: 10.1002/mnfr.201700754
- Luo, T., Wagner, E., Crandall, J. E., and Dräger, U. C. (2004). A retinoic-acid critical period in the early postnatal mouse brain. *Biol. Psychiatry* 56, 971–980. doi: 10.1016/j.biopsych.2004.09.020
- Ma, K., Qin, L., Matas, E., Duffney, L. J., Liu, A., and Yan, Z. (2018). Histone deacetylase inhibitor MS-275 restores social and synaptic function in a Shank3-deficient mouse model of autism. *Neuropsychopharmacology* 43, 1779–1788. doi: 10.1038/s41386-018-0073-1
- Mabunga, D. F., Gonzales, E. L., Kim, J. W., Kim, K. C., and Shin, C. Y. (2015). Exploring the validity of valproic acid animal model of autism. *Exp. Neurobiol.* 24, 285–300. doi: 10.5607/en.2015.24.4.285
- Maden, M., and Holder, N. (1991). The involvement of retinoic acid in the development of the vertebrate central nervous system. *Dev. Suppl. Suppl* 2, 87–94.
- Markram, K., Rinaldi, T., La Mendola, D., Sandi, C., and Markram, H. (2008). Abnormal fear conditioning and amygdala processing in an animal model of autism. *Neuropsychopharmacology* 33, 901–912. doi: 10.1038/sj.npp.1301453
- Nicolini, C., and Fahnstock, M. (2018). The valproic acid-induced rodent model of autism. *Exp. Neurol.* 299, 217–227. doi: 10.1016/j.expneurol.2017.04.017
- Phiel, C. J., Zhang, F., Huang, E. Y., Guenther, M. G., Lazar, M. A., and Klein, P. S. (2001). Histone deacetylase is a direct target of valproic acid, a potent anticonvulsant, mood stabilizer, and teratogen. *J. Biol. Chem.* 276, 36734–36741. doi: 10.1074/jbc.M101287200
- Poon, M. M., and Chen, L. (2008). Retinoic acid-gated sequence-specific translational control by RARalpha. *Proc. Natl. Acad. Sci. U.S.A.* 105, 20303–20308. doi: 10.1073/pnas.0807740105
- Rasalam, A. D., Hailey, H., Williams, J. H., Moore, S. J., Turnpenny, P. D., Lloyd, D. J., et al. (2005). Characteristics of fetal anticonvulsant syndrome associated autistic disorder. *Dev. Med. Child. Neurol.* 47, 551–555. doi: 10.1017/s0012162205001076
- Rinaldi, T., Kulangara, K., Antonello, K., and Markram, H. (2007). Elevated NMDA receptor levels and enhanced postsynaptic long-term potentiation induced by prenatal exposure to valproic acid. *Proc. Natl. Acad. Sci. U.S.A.* 104, 13501–13506. doi: 10.1073/pnas.0704391104
- Rylaarsdam, L., and Gumez-Gamboa, A. (2019). Genetic causes and modifiers of autism spectrum disorder. *Front. Cell Neurosci.* 13:385. doi: 10.3389/fncel.2019.00385
- Schilderink, R., Verseijden, C., Seppen, J., Muncan, V., van den Brink, G. R., Lambers, T. T., et al. (2016). The SCFA butyrate stimulates the epithelial production of retinoic acid via inhibition of epithelial HDAC. *Am. J. Physiol. Gastrointest. Liver Physiol.* 310, G1138–G1146. doi: 10.1152/ajpgi.00411.2015
- Siegenthaler, J. A., Ashique, A. M., Zarbalis, K., Patterson, K. P., Hecht, J. H., Kane, M. A., et al. (2009). Retinoic acid from the meninges regulates cortical neuron generation. *Cell* 139, 597–609. doi: 10.1016/j.cell.2009.10.004
- Simonini, M. V., Camargo, L. M., Dong, E., Maloku, E., Veldic, M., Costa, E., et al. (2006). The benzamide MS-275 is a potent, long-lasting brain region-selective inhibitor of histone deacetylases. *Proc. Natl. Acad. Sci. U.S.A.* 103, 1587–1592. doi: 10.1073/pnas.0510341103
- Smith, V., and Brown, N. (2014). Prenatal valproate exposure and risk of autism spectrum disorders and childhood autism. *Arch. Dis. Child. Educ. Pract. Ed* 99:198. doi: 10.1136/archdischild-2013-305636
- Sorrell, J. M. (2013). Diagnostic and statistical manual of mental disorders-5: implications for older adults and their families. *J. Psychosoc. Nurs. Ment. Health Serv.* 51, 19–22. doi: 10.3928/02793695-20130207-01
- Wan, C., Shi, Y., Zhao, X., Tang, W., Zhang, M., Ji, B., et al. (2009). Positive association between ALDH1A2 and schizophrenia in the Chinese population. *Prog. Neuropsychopharmacol. Biol. Psychiatry* 33, 1491–1495. doi: 10.1016/j.pnpbp.2009.08.008

- Xu, X., Li, C., Gao, X., Xia, K., Guo, H., Li, Y., et al. (2018). Excessive UBE3A dosage impairs retinoic acid signaling and synaptic plasticity in autism spectrum disorders. *Cell Res.* 28, 48–68. doi: 10.1038/cr.2017.132
- Xu, Z. H., Yang, Q., Feng, B., Liu, S. B., Zhang, N., Xing, J. H., et al. (2012). Group I mGluR antagonist rescues the deficit of D1-induced LTP in a mouse model of fragile X syndrome. *Mol. Neurodegener.* 7:24. doi: 10.1186/1750-1326-7-24
- Yoshino, J., Akiyama, Y., Shimada, S., Ogura, T., Ogawa, K., Ono, H., et al. (2020). Loss of ARID1A induces a stemness gene ALDH1A1 expression with histone acetylation in the malignant subtype of cholangiocarcinoma. *Carcinogenesis* 41, 734–742. doi: 10.1093/carcin/bgz179
- Zhang, X., Chen, K., Chen, J., Liu, Y. X., Qu, P., and Li, T. Y. (2011). Effect of marginal vitamin A deficiency during pregnancy on retinoic acid receptors and N-methyl-D-aspartate receptor expression in the offspring of rats. *J. Nutr. Biochem.* 22, 1112–1120. doi: 10.1016/j.jnutbio.2010.09.010
- Zhang, X., Yuan, X., Chen, L., Wei, H., Chen, J., and Li, T. (2017). The change in retinoic acid receptor signaling induced by prenatal marginal vitamin A deficiency and its effects on learning and memory. *J. Nutr. Biochem.* 47, 75–85. doi: 10.1016/j.jnutbio.2017.05.007
- Zoghbi, H. Y. (2003). Postnatal neurodevelopmental disorders: meeting at the synapse? *Science* 302, 826–830. doi: 10.1126/science.1089071
- Zoghbi, H. Y., and Bear, M. F. (2012). Synaptic dysfunction in neurodevelopmental disorders associated with autism and intellectual disabilities. *Cold Spring Harb. Perspect. Biol.* 4:a009886. doi: 10.1101/cshperspect.a009886

Conflict of Interest: The authors declare that the research was conducted in the absence of any commercial or financial relationships that could be construed as a potential conflict of interest.

Copyright © 2021 Liu, Tan, Cheng, Wang, Xiao, Zhu, Wu, Lai, Zhang, Chen and Li. This is an open-access article distributed under the terms of the Creative Commons Attribution License (CC BY). The use, distribution or reproduction in other forums is permitted, provided the original author(s) and the copyright owner(s) are credited and that the original publication in this journal is cited, in accordance with accepted academic practice. No use, distribution or reproduction is permitted which does not comply with these terms.